Calibration of an Articulated Camera System

CHEN Junzhou and Kin Hong WONG

Department of Computer Science and Engineering

The Chinese University of Hong Kong

{jzchen, khwong}@cse.cuhk.edu.hk

Abstract

Multiple Camera Systems (MCS) have been widely used in many vision applications and attracted much attention recently. There are two principle types of MCS, one is the Rigid Multiple Camera System (RMCS); the other is the Articulated Camera System (ACS). In an RMCS, the relative poses (relative 3-D position and orientation) between the cameras are invariant. While, in an ACS, the cameras are articulated through movable joints, the relative pose between them may change. Therefore, through calibration of an ACS we want to find not only the relative poses between the cameras but also the positions of the joints in the ACS.

Although calibration methods for RMCS have been extensively developed during the past decades, the studies of ACS calibration are still rare. In this paper, two ACS calibration methods are proposed. The first one uses the feature correspondences between the cameras in the ACS. The second one requires only the ego-motion information of the cameras and can be used for the calibration of the non-overlapping view ACS. In both methods, the ACS is assumed to have performed general transformations in a static environment. The efficiency and robustness of the proposed methods are tested by simulation and real experiments. In the real experiment, the intrinsic and extrinsic parameters of the ACS are calibrated using the same image sequences, no extra data capturing step is required. The corresponding trajectory is recovered and illustrated using the calibration results of the ACS. To our knowledge, we are the first to study the calibration of ACS.

1. Introduction

Calibration of a Multiple Camera System (MCS) is an essential step in many computer vision tasks such as SLAM (Simultaneous Localization and Map), surveillance, stereo and metrology [11, 3, 7, 12]. Both the intrinsic and extrinsic parameters of the MCS are required to be estimated before the MCS can be used. The intrinsic parameters [9] describe the internal camera geometric and optical character-
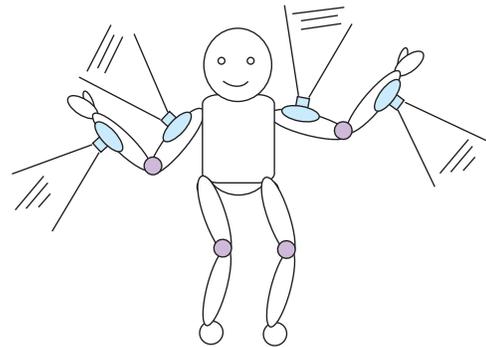

Figure 1. An Robot with Four Cameras Attached on It, Where the Cameras are Articulated.

istics of each camera in the MCS. In a Rigid Multiple Camera System (RMCS), the cameras are fixed to each other. The extrinsic parameters [5] of an RMCS describe the relative pose (the relative 3-D position and orientation, totally, six degrees of freedom) between the cameras in the MCS. Calibration methods of the intrinsic parameters of a camera are well established [15, 9]. Calibration methods for the extrinsic parameters of an RMCS are also widely studied. For instance, Maas proposed an automatic RMCS calibration technique with a moving reference bar which can be seen by all cameras [13]. Antone and Teller developed an algorithm which recovers the relative poses of cameras by overlapping portions of the outdoor scene [1]. Baker and Aloimonos presented RMCS calibration methods using calibration objects such as a wand with LEDs or a rigid board with known patterns [2, 4]. Dornaika proposed a stereo rig self-calibration method by the monocular epipolar geometries and geometric constraints of a moving RMCS, in which only the feature correspondences between the monocular images of each camera are required [8]. In hand-eye calibration, it is demonstrated that when a sensor is mounted on a moving robot hand, the relationship between the sensor coordinate system and hand coordinate system can be calculated by the motion information of the hand and the sensor [10]. One example of using kinematic information of the cameras for RMCS is discussed by Caspi and Irani

[6], they indicated that if the cameras of a non-overlapping view RMCS are close to each other and share a same projection center, their recorded image sequences can be aligned effectively by the estimated transformations inside each image sequence.

However, in some types of MCS, the relative poses between the cameras are not fixed, hence the calibration methods for the RMCS cannot be used directly. In Figure 1, a novel application of limb pose estimation by attaching cameras on the arms of a robot is shown. On each arm of the robot, two cameras are articulated to each other through the elbow joint of the arm. When the robot moves, the relative pose between the cameras may change, while, the coordinate of the elbow joint refers to each camera attached on the corresponding arm is invariant. In this paper, such a type of MCS is named as Articulated Camera System (ACS). The joint of the elbow is named as the *joint* in the ACS.

ACSs can be easily found in the real world, such as camera systems attached on human, robots and animals. Before using an ACS, it has to be calibrated. However, there are still some unsolved problems: (i) In an ACS with overlapping view, traditional calibration methods cannot estimate the positions of the joints in the ACS. (ii) In a non-overlapping view ACS, neither the positions of the joints in the ACS nor the relative poses between the cameras in the ACS can be estimated by traditional calibration methods.

These considerations in mind motivate us to develop the technologies in this paper. The rest of this paper are organized as follows: Section 2 and 3 analysis the constraints in a moving ACS. The corresponding calibration methods are proposed. Section 4 and 5 evaluate the proposed method by simulation and real experiment. In section 6, a brief conclusion and the future plan are presented.

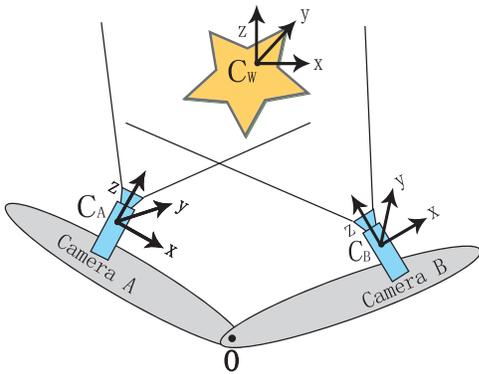## 2. Calibration of ACS with Overlapping Views

Figure 2. An Articulated Camera System with Overlapping Views

Suppose two rigid objects are articulated at joint O and two cameras (camera A and B) are fixed on the two rigid objects respectively (See Figure 2). Let C_A be the coordinate system of camera A, C_B the coordinate system of camera B. Suppose there are enough feature correspondences between the cameras so that the pose of C_A and C_B referring to the same coordinate system C_W can be estimated. Therefore, the relative pose between C_A and C_B is known. We want to find the position of O in the ACS. Let $\mathbf{H}_{AW}$ and $\mathbf{H}_{BW}$ be the Euclidean transformation matrixes describe the C_A and C_B refer to C_W, so that for any point P:

$$P_A = \mathbf{H}_{AW} P_W = \begin{bmatrix} \mathbf{R}_{AW} & T_{AW} \\ 0 & 1 \end{bmatrix} P_W \quad (1)$$

$$P_B = \mathbf{H}_{BW} P_W = \begin{bmatrix} \mathbf{R}_{BW} & T_{BW} \\ 0 & 1 \end{bmatrix} P_W \quad (2)$$

, where $\mathbf{R}$ is the 3×3 rotation matrix, T is 3×1 vector, P_W, P_A and P_B are the homogenous coordinates of the 3-D Point P refer to C_W, C_A and C_B respectively.

According to equations (1) and (2):

$$P_W = \mathbf{H}_{AW}^{-1} P_A = \mathbf{H}_{BW}^{-1} P_B \quad (3)$$

$$\mathbf{H}_{AW}^{-1} P_A - \mathbf{H}_{BW}^{-1} P_B = 0 \quad (4)$$

$$\begin{bmatrix} \mathbf{R}_{AW}^T & -\mathbf{R}_{AW}^T T_{AW} \\ 0 & 1 \end{bmatrix} \begin{bmatrix} \bar{P}_A \\ 1 \end{bmatrix} - \begin{bmatrix} \mathbf{R}_{BW}^T & -\mathbf{R}_{BW}^T T_{BW} \\ 0 & 1 \end{bmatrix} \begin{bmatrix} \bar{P}_B \\ 1 \end{bmatrix} = 0 \quad (5)$$

$$\mathbf{R}_{AW}^T \bar{P}_A - \mathbf{R}_{BW}^T \bar{P}_B = \mathbf{R}_{AW}^T T_{AW} - \mathbf{R}_{BW}^T T_{BW} \quad (6)$$

, where $\mathbf{R}^T$ is the transpose of $\mathbf{R}$. Suppose the ACS performed n transformations, for the i-th transformation of the ACS, according to equation (6):

$$(\mathbf{R}_{AW}^i)^T \bar{P}_A - (\mathbf{R}_{BW}^i)^T \bar{P}_B = (\mathbf{R}_{AW}^i)^T T_{AW}^i - (\mathbf{R}_{BW}^i)^T T_{BW}^i \quad (7)$$

Let $\tilde{O} = \begin{bmatrix} \bar{O}_A^T & \bar{O}_B^T \end{bmatrix}^T$, where $\bar{O}_A$ and $\bar{O}_B$ are the coordinates of the joint O refer to C_A and C_B respectively. Equation (7) can be rewritten as:

$$\begin{bmatrix} (\mathbf{R}_{AW}^i)^T & -(\mathbf{R}_{BW}^i)^T \end{bmatrix} \tilde{O} = (\mathbf{R}_{AW}^i)^T T_{AW}^i - (\mathbf{R}_{BW}^i)^T T_{BW}^i \quad (8)$$

Since camera A and B are fixed on the articulated rigid objects, $\tilde{O}$ is invariant during the transformation of the ACS. The transformations ($\mathbf{R}_{AW}^i$, $\mathbf{R}_{BW}^i$, T_{AW}^i and T_{BW}^i for $i \in [1 \ldots n]$) of the camera coordinate systems are calculated by the projected image sequences. We propose that $\tilde{O}$ can be estimated by a least squares method, when the ACS has moved to many different positions and captured enough samples of $\mathbf{R}_{AW}^i$, $\mathbf{R}_{BW}^i$, T_{AW}^i and T_{BW}^i.
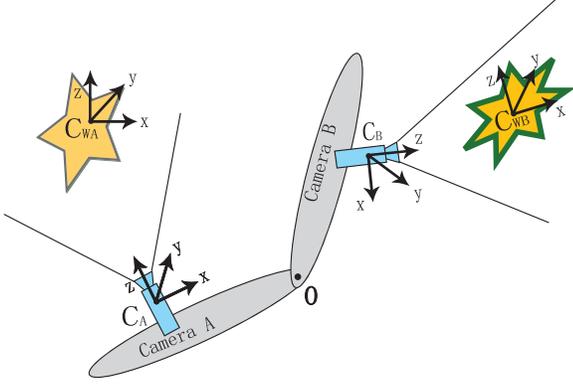
Figure 3. A Non-overlapping View Articulated Camera System

3. Calibration of Non-Overlapping View ACS

In many situations, there is no overlapping view between the cameras in an ACS. And the lack of common features makes the calibration method proposed in section 2 become invalid (See Figure 3). Moreover, since the relative pose between the cameras in the ACS cannot be estimated by the overlapping views, the calibration of the relative poses between the non-overlapping view cameras is also required. In this section, a calibration method based on the ego-motion information of the cameras in an ACS is discussed.

3.1. Recovering the Position of the Joint Refers to the Cameras in the ACS

Let C_A^{init} and C_B^{init} be the coordinate systems of camera A and B respectively at the initial state (time $t = 0$). Suppose the ACS performs n transformations. Since the coordinate of the joint O refers to camera A is fixed during the transformation of the ACS. At time $t = i$, we have:

$$O_A^i = \mathbf{H}_A^i O_A = \begin{bmatrix} \mathbf{R}_A^i & T_A^i \\ 0 & 1 \end{bmatrix} O_A \qquad (9)$$

, where $\mathbf{H}_A^i$ is the Euclidean transformation matrix of camera A at time i refers to C_A^{init}. $\mathbf{R}_A^i$ and T_A^i describe the orientation and origin of camera A at time i refer to C_A^{init}. Also O_A is the coordinate of point O at initial state refers to C_A^{init}, and O_A^i is the coordinate of point O at time i refers to C_A^{init}.

If the position of the joint O refers to C_A^{init} is fixed during the transformations of the ACS, we have: $O_A^i = O_A$, $\forall i \in [1, \ldots, n]$. For i-th transformation of the ACS, according to equation (9):

$$O_A = \mathbf{H}_A^i O_A = \begin{bmatrix} \mathbf{R}_A^i & T_A^i \\ 0 & 1 \end{bmatrix} O_A \qquad (10)$$

$$(\mathbf{R}_A^i - I)\bar{O}_A = -T_A^i \qquad (11)$$

Let $\mathbf{M}_A = [(\mathbf{R}_A^1 - I)^T, (\mathbf{R}_A^2 - I)^T, \ldots, (\mathbf{R}_A^n - I)^T]^T$, $\tilde{T}_A = [(T_A^1)^T, (T_A^2)^T, \ldots, (T_A^n)^T]^T$, we have:

$$\mathbf{M}_A \bar{O}_A = -\tilde{T}_A \qquad (12)$$

Since the transformations ($\mathbf{R}_A^i$ and T_A^i, $\forall i \in [1 \ldots n]$) of camera A can be calculated by the projected image sequence. We propose $\bar{O}_A$ can be estimated by a least squares method. Similarly, $\bar{O}_B$ can also be estimated. Therefore, O_A and O_B are recovered.

3.2. The Uniqueness of the Joint Pose Estimation

If the different segments of the articulated camera system (ACS) are connected by 1D rotational joints (connected by point rotational joints) and the ACS can perform general transformations, the solution of the joint pose estimation is unique:

For the joint pose estimation method using special motion (in section 3.1). Suppose the solution of the joint pose estimation is not unique, there must exist at lest two different 3D points O_1 and O_2 satisfy equation (12). We have: $\mathbf{M}_A O_1 = -\tilde{T}_A$ and $\mathbf{M}_A O_2 = -\tilde{T}_A$. Therefore, any point $P = sO_1 + (1 - s)O_2$ will also satisfy equation (12), where s is an arbitrary scalar. According to the definition of P, P is the point on the line passing through the points O_1 and O_2. Since P satisfy equation (12) represents that the position of the P refers to the camera in the ACS is invariant during the transformation of the ACS, it means the different segments of ACS are connected by the 2D rotational axis instead of the 1D rotational joints. The position of the points on the 2D rotational axis refer to the camera in the ACS is invariant during the transformation of the ACS. However, it conflicts with the assumption. Similarly, the uniqueness of the joint pose estimation method using overlapping views (in section 2) can also be verified.

3.3. Recovering the Relative Pose Between the Cameras of the Non-overlapping view ACS

Let $\mathbf{H}_{BA}$ be the Euclidean transformation matrix between C_A^{init} and C_B^{init}, so that for any point P:

$$P_B = \mathbf{H}_{BA} P_A = \begin{bmatrix} \mathbf{R}_{BA} & T_{BA} \\ 0 & 1 \end{bmatrix} P_A = \mathbf{H}_{BA} P_A \quad (13)$$

, where P_A and P_B are the homogenous coordinate of Point P refer to C_A^{init} and C_B^{init} respectively.

The relative pose ($\tilde{\mathbf{R}}_{BA}$ and $\tilde{T}_{BA}$) between C_A^{init} and C_B^{init} is defined as:

$$\tilde{\mathbf{R}}_{BA} = \mathbf{R}_{BA}^T \qquad (14)$$

$$\tilde{T}_{BA} = -\mathbf{R}_{BA}^T T_{BA} \qquad (15)$$

Let O_B^i be the coordinate of joint O at time i refer to C_B^{init}. Since the coordinate of the joint O refer to camera B is invariant:

$$
\begin{aligned}
O_B^i &= \left[\begin{array}{cc} \mathbf{R}_B^i & T_B^i \\ 0 & 1 \end{array} \right] O_B \\
&= \left[\begin{array}{cc} \mathbf{R}_B^i & T_B^i \\ 0 & 1 \end{array} \right] \left[\begin{array}{cc} \mathbf{R}_{BA} & T_{BA} \\ 0 & 1 \end{array} \right] O_A \\
&= \left[\begin{array}{cc} \mathbf{R}_B^i \mathbf{R}_{BA} & \mathbf{R}_B^i T_{BA} + T_B^i \\ 0 & 1 \end{array} \right] O_A \quad (16)
\end{aligned}
$$

According to equations (9) and (13):

$$
\begin{aligned}
O_B^i &= \mathbf{H}_{BA} O_A^i \\
&= \left[\begin{array}{cc} \mathbf{R}_{BA} & T_{BA} \\ 0 & 1 \end{array} \right] \left[\begin{array}{cc} \mathbf{R}_A^i & T_A^i \\ 0 & 1 \end{array} \right] O_A \\
&= \left[\begin{array}{cc} \mathbf{R}_{BA} \mathbf{R}_A^i & \mathbf{R}_{BA} T_A^i + T_{BA} \\ 0 & 1 \end{array} \right] O_A \quad (17)
\end{aligned}
$$

According to equations (16) and (17):

$$
\begin{aligned}
&\left[\begin{array}{cc} \mathbf{R}_B^i \mathbf{R}_{BA} & \mathbf{R}_B^i T_{BA} + T_B^i \\ 0 & 1 \end{array} \right] \left[\begin{array}{c} \bar{O}_A \\ 1 \end{array} \right] \\
&= \left[\begin{array}{cc} \mathbf{R}_{BA} \mathbf{R}_A^i & \mathbf{R}_{BA} T_A^i + T_{BA} \\ 0 & 1 \end{array} \right] \left[\begin{array}{c} \bar{O}_A \\ 1 \end{array} \right] \quad (18)
\end{aligned}
$$

$$
\begin{aligned}
&\left[\begin{array}{c} \mathbf{R}_B^i \mathbf{R}_{BA} \bar{O}_A + \mathbf{R}_B^i T_{BA} + T_B^i \\ 1 \end{array} \right] \\
&= \left[\begin{array}{c} \mathbf{R}_{BA} \mathbf{R}_A^i \bar{O}_A + \mathbf{R}_{BA} T_A^i + T_{BA} \\ 1 \end{array} \right] \quad (19)
\end{aligned}
$$

$$
\begin{aligned}
\mathbf{R}_B^i \mathbf{R}_{BA} \bar{O}_A + \mathbf{R}_B^i T_{BA} - \mathbf{R}_{BA} \mathbf{R}_A^i \bar{O}_A & \\
- \mathbf{R}_{BA} T_A^i + T_B^i - T_{BA} &= 0 \quad (20)
\end{aligned}
$$

Since $\bar{O}_A$ can be estimated by the method discussed in section 3.3, the $\mathbf{R}_{BA}$ and T_{BA} can be estimated by a least square method, when the ACS perform enough general motions.

In our simulation and real experiment, the estimated R_{BA} is refined by a method discussed in [14]. Then the roll, pitch and yaw corresponding to the R_{BA} are estimated according to the definition of the rotation matrix [9]. Let $R_{BA} = M(r, p, y)$, where r p and y are the corresponding roll, pitch and yaw of $\mathbf{R}_{BA}$, M is a function from roll, pitch and yaw to the corresponding rotation matrix. Then, the r, p, y, T_{BA} and $\bar{O}_A$ are optimized by minimizing the nonlinear error function:

$$
\begin{aligned}
E(r, p, y, T_{BA}, O_A) = \sum_{i=1}^{n} (\mathbf{R}_B^i M(r, p, y) \bar{O}_A + \mathbf{R}_B^i T_{BA} \\
- M(r, p, y) \mathbf{R}_A^i \bar{O}_A - M(r, p, y) T_A^i + T_B^i - T_{BA}) \quad (21)
\end{aligned}
$$

using a Levenberg-Marquardt method. Finally, the R_{BA} is recovered from the optimized r, p and y. The relative pose between the C_A^{init} and C_B^{init} is calculated by equations (14) and (15).

4. Simulation

In this section, the proposed calibration methods are evaluated with synthetic transformation data.

4.1. Performance w.r.t. Noise in Transformation Data

Setup and Notations: In each test, one ACS with 2 cameras and 1 joint is generated randomly. In which, $1 \leq |O_A| \leq 2$ meters, $1 \leq |O_B| \leq 2$ meters. The generated ACS performs 30 random transformations.

Performance of the Calibration Method for ACS with Overlapping Views: In the first simulation, the proposed algorithm is tested 100 times. Zero mean Gaussian noise is added to the transformation data of the cameras. The configuration, input and output of our simulation system are list as Table 1. Since we assume there are overlapping views between the two cameras, the relative pose between them can be estimated by many existing methods as discussed in section 1. Only the performance of joint pose estimation is evaluated in our simulation. The error of joint estimation are computed by:

$$
Err = \frac{|\bar{O}_A - \hat{O}_A|}{2|\bar{O}_A|} + \frac{|\bar{O}_B - \hat{O}_B|}{2|\bar{O}_B|} \quad (22)
$$

, where $\bar{O}_A$ is the ground truth, $\hat{O}_A$ is the estimated position of joint O refer to camera A. Similarly, $\bar{O}_B$ is the ground truth, $\hat{O}_B$ is the estimated position of joint O refer to camera B. The corresponding results are shown in Figure 4 and 5.

Table 1. Configuration, Input and Output

Configuration	
No. of Cameras in the ACS	2
No. of Joints in the ACS	1
Random transformations per test (n)	30
Number of tests	100
Input ($i = 1 \ldots n$)	
Rotations of cameras ($\mathbf{R}_{AW}^i, \mathbf{R}_{BW}^i$)	$2 \times 30 \times 100$
Translations of cameras (T_{AW}^i, T_{BW}^i)	$2 \times 30 \times 100$
Zero Mean Gaussian noise:	
$0 \leq \sigma_{rot} \leq 2.4°$ and $0 \leq \sigma_{trans} \leq 0.1 meters$	
Output	
Mean error of joint pose estimation	
STD error of joint pose estimation	

Performance of the Calibration Method for Non-Overlapping Views ACS: In the second simulation, firstly, the pose of the joint is fixed refers to C_A^{init} during the transformations of the ACS. The pose of the joint refers to the camera A (O_A) is calibrated by the transformations of camera A. Similarly, O_B is calibrated. Then, the ACS performs several general transformations (the joint is not needed to
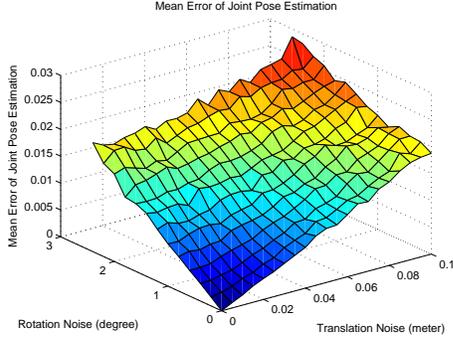
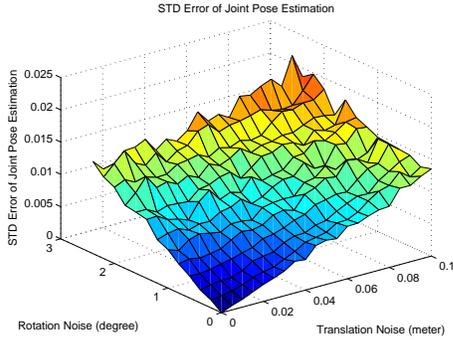Figure 4. Mean Error of Joint Position Estimation

Figure 5. STD Error of Joint Position Estimation

Table 2. Configuration, Input and Output

Configuration	
No. of Cameras in the ACS	2
No. of Joints in the ACS	1
Random transformations per test (n)	30
Number of tests	100
Input ($i = 1 \dots n$)	
Transformations with fixed joint pose:	
Rotations of cameras ($\mathbf{R}_A^i, \mathbf{R}_B^i$)	$2 \times 30 \times 100$
Translations of cameras (T_A^i, T_B^i)	$2 \times 30 \times 100$
General transformations:	
Rotations of cameras ($\mathbf{R}_A^i, \mathbf{R}_B^i$)	$2 \times 30 \times 100$
Translations of cameras (T_A^i, T_B^i)	$2 \times 30 \times 100$
Zero Mean Gaussian noise:	
$0 \le \sigma_{rot} \le 2.4°$ and $0 \le \sigma_{trans} \le 0.1 meters$	
Output	
Mean error of joint pose estimation	
STD error of joint pose estimation	
Mean error of relative translation estimation	
STD error of relative translation estimation	
Mean error of relative rotation estimation	
STD error of relative rotation estimation	

be fixed refer to C_A^{init}), the relative pose between the cameras are calibrated using the estimated joint pose and the transformations of the cameras. The configuration, input and output of the simulation system are listed as Table 2. The error of joint pose, relative rotation, relative translation estimation are calculated by equation (22), (23) and (24) respectively.

Figure 6 and 7 show the results of joint pose estimation. Compare with the calibration method using the overlapping views, the calibration method using special motions is more accurate. The mean and STD error of the relative rotation and translation estimation are presented in Figure 8, 9, 10 and 11. The proposed algorithms are shown to be stable, when the zero mean Gaussian noise from $0°$ to $2.4°$ is added to the roll, pitch and yaw of the rotation data, and the zero mean Gaussian noise from 0 to 0.1 meters is added to the translation data.

$$Err = \sqrt{|roll - \widehat{roll}|^2 + |pitch - \widehat{pitch}|^2 + |yaw - \widehat{yaw}|^2} \tag{23}$$

$$Err = \frac{|T_{AB} - \hat{T}_{AB}|}{|T_{AB}|} \tag{24}$$
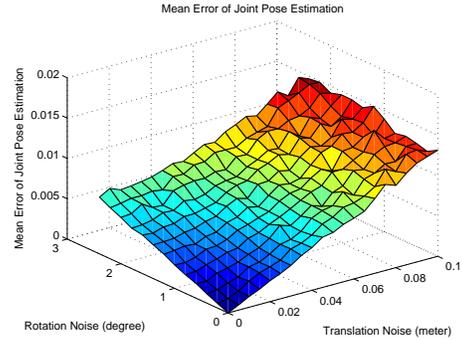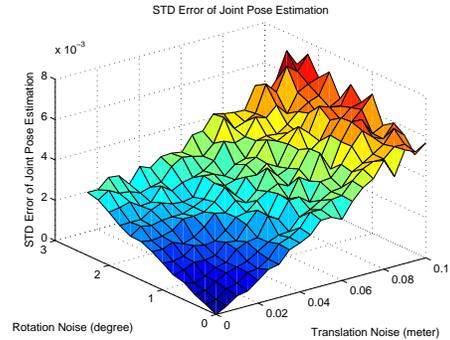

Figure 6. Mean Error of Joint Position Estimation
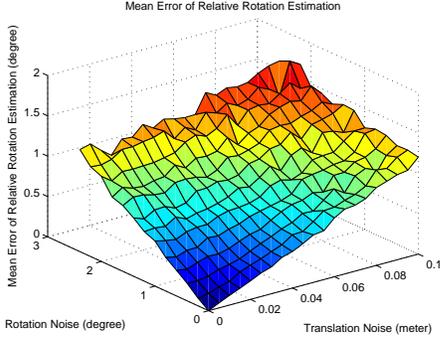

Figure 7. STD Error of Joint Position Estimation

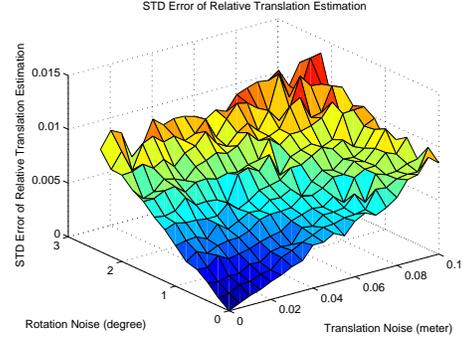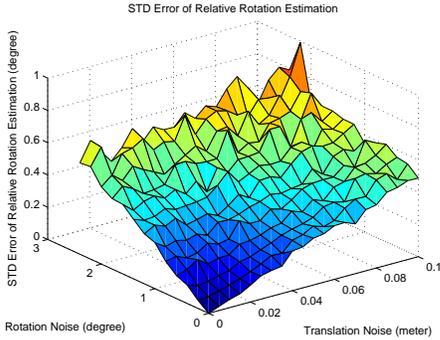Figure 8. Mean Error of Relative Rotation Estimation

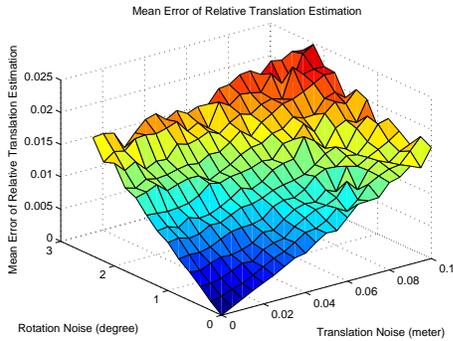Figure 9. STD Error of Relative Rotation Estimation

Figure 10. Mean Error of Relative Translation Estimation

5. Real Experiment

In the real experiments, an ACS with two cameras (*Cannon PowerShot G9*) is set up as Figure 13 (a). The intrinsic parameters of each camera in the ACS are calibrated by Bouguet's implementation ("Camera Calibration Toolbox for Matlab") of [15]. Since the Bouguet's Toolbox can also estimate the pose information of the camera, the transformations of each camera are calculated using the same image sequence for the intrinsic calibration simultaneously. No additional images nor manual input is required in the real experiments.

Figure 11. STD Error of Relative Translation Estimation

5.1. Calibration of the Pose of the Joint in Each Camera

By Overlapping Views (Algorithm I): In the first real experiment, the two cameras in the ACS observe the same checker plane and record images simultaneously. The two cameras are free to move during the transformation of the ACS. Two image sequences (Q_1 and Q_2) are recorded, each sequence consists of 15 images of size 1600×1200. The estimated joint pose are list in Table 3 as algorithm I.

By Fixed-Joint Motions (Algorithm II): In the second real experiment, the joint of the ACS is fixed refers to the world coordinate system during the transformation of the ACS. The two cameras do not need to view the same checker plane. And each camera records the image sequence independently. Two image sequences (Q_3 and Q_4) are recorded, each sequence consists of 12 images of size 1600×1200. The camera pose of the first image is selected as the initial pose to generate the transformation sequence of each camera. The estimated joint pose are list in Table 3 as algorithm II. The poses of the joint refer to the two cameras in the ACS are also estimated manually for comparison purpose. Since the camera pose of any image in each image sequence can be chosen as the initial camera pose (see section 3.1), the proposed algorithm is also tested by choosing different images as the reference. The mean and standard derivation of the corresponding calibration results are presented in Table 4.

5.2. Calibration of Relative Pose Between the Cameras in the Non-Overlapping View ACS (Algorithm III)

In the third real experiment, firstly, we use the non-overlapping view ACS calibration method to process the image sequences Q_1 and Q_2. The joint pose ($\bar{O}_A$) estimated by algorithm II is used as the input for the relative pose calibration. Since there are overlapping views between Q_1 and Q_2, we also calibrate the relative pose between the two cameras by the feature correspondences for compari-

Table 3. Results Of Joint Pose Calibration
I: the algorithm using overlapping views. II: the algorithm using fixed-joint motions. M: manual measurement(ground truth). O_A is the coordinate of the joint refers to camera A, the same applies to O_B.

Algorithm		Joint Pose (mm)		
		X	Y	Z
I	O_A	300.28	50.07	-33.47
	O_B	-273.70	53.81	-30.15
II	O_A	304.55	47.64	-37.66
	O_B	-265	54.41	-35.48
M	O_A	300 ± 10	50 ± 10	-40 ± 10
	O_B	-270 ± 10	50 ± 10	-30 ± 10

Table 4. Mean and STD of the Joint Pose Calibration Algorithm II Using Different Reference Images. (O_A is the coordinate of the joint refers to camera A, the same applies to O_B.)

Algorithm		Joint Pose (mm)		
II		X	Y	Z
Mean	O_A	305.44	47.19	-39.2
	O_B	-262.97	56.21	-39.20
STD	O_A	1.89	1.16	3.02
	O_B	3.3	2.67	2.58

son. The calibration result are listed in Table 5. After the joint pose refers to each camera in the ACS and relative pose between the cameras in the ACS are calibrated, the trajectory of the ACS is recovered (see Figure 12). The proposed

Table 5. Result of Relative Pose Calibration
III: our method. F: using feature correspondences.

Algorithm	Relative Rotation (Degree)		
	Roll	Pitch	Yaw
III	17.7158	-11.3660	-80.1913
F	17.5459	-10.6024	-78.9854

Algorithm	Relative Translation (mm)		
	T_x	T_y	T_z
III	295.4183	-232.4576	34.5004
F	294.0235	-229.8369	28.9739

calibration method is also tested by non-overlapping view image sequences. Figure 13 (b), (c), (d) shows the configuration of the non-overlapping view ACS calibration system in the real experiment. Two image sequences (Q_5 and Q_6) are recorded, each sequence consists of 17 images of size 1600×1200. There is no overlapping view between Q_5 and Q_6. Figure 14 shows some samples of the recorded images. We also manually measured the relative pose between the two cameras for comparison. Since no feature correspondence can be used, we only get a rough estimation by a ruler. The calibration results are shown in Table 6. After the relative pose between the cameras at the initial state is estimated, the trajectory of the non-overlapping view ACS is recovered (see Figure 15).
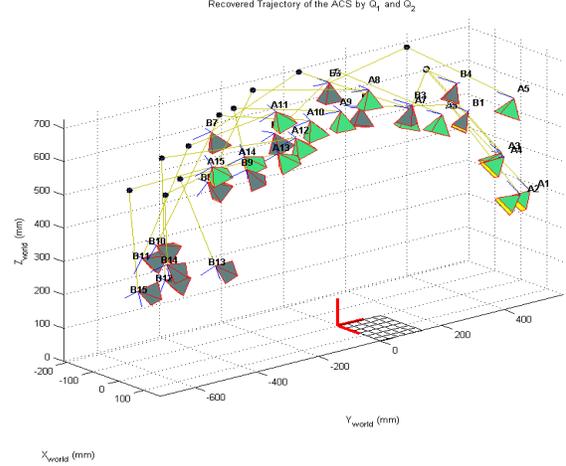

Figure 12. The Trajectory of the ACS Recovered from Q_1 and Q_2
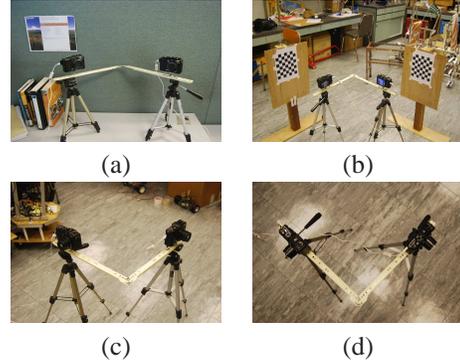

(a)   (b)

(c)   (d)

Figure 13. The ACS with Two Cannon PowerShot G9 Used in the Real Experiment. (a) The ACS Used in the Real Experiment. (b) The ACS and two Checker Planes. (c) In the Front of the ACS. (d) On the Top of the ACS.
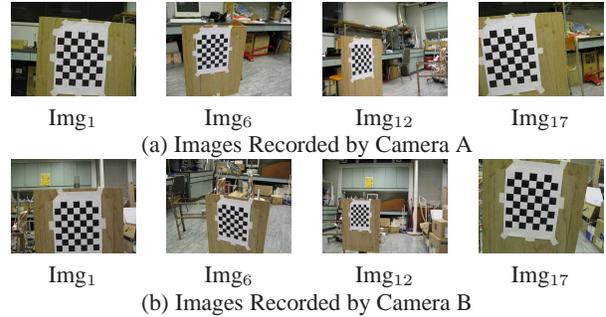

Img_1 Img_6 Img_{12} Img_{17}
(a) Images Recorded by Camera A

Img_1 Img_6 Img_{12} Img_{17}
(b) Images Recorded by Camera B
Figure 14. Images Recorded by the ACS

6. Conclusion

In this paper, an ACS calibration method is developed. Both the simulation and real experiment show that the pose of the joint in an ACS can be estimated robustly. When there is no overlapping view between the cameras in an ACS, the joint pose and the relative pose between the cameras can also be calculated. The trajectory of an ACS can be recov-

Table 6. Result of Relative Pose Calibration Using Non-Overlapping View Image Sequences. (III: our method. M: manual measurement.)

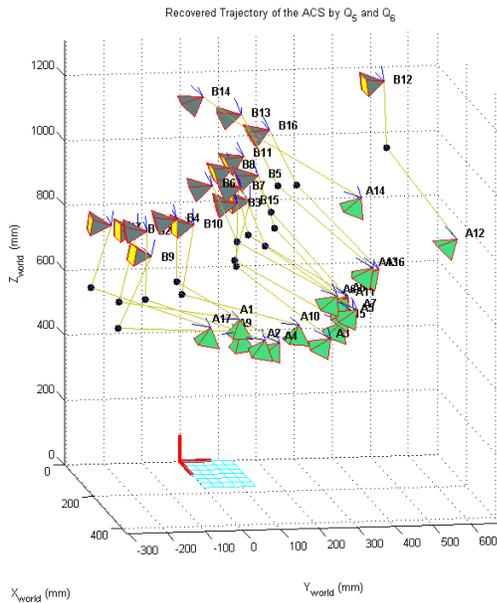| Algorithm	Relative Rotation (Degree)		
	Roll	Pitch	Yaw
III	1.3182	88.4530	0.7315
M	0 ± 5	90 ± 5	0 ± 5
Algorithm	Relative Translation (mm)		
	T_x	T_y	T_z
III	291.3321	-17.2837	-292.1382
M	290±20	0 ± 20	280 ±20

Figure 15. The Trajectory of the ACS Recovered from Q_5 and Q_6

ered after the ACS is calibrated. The proposed calibration method requires only the image sequences recorded by the cameras in the ACS. In the real experiment, the intrinsic and extrinsic parameters of the ACS are calibrated using the same image sequences simultaneously.

Our future plan may focus on using an ACS attached on different parts of human body to track the motion of the human. We foresee that if calibration of articulated cameras become a simple routine, researchers will find many novel and interesting applications for such a camera system.

References

[1] M. Antone and S. Teller. Scalable extrinsic calibration of omni-directional image networks. *International Journal of Computer Vision*, 49(2):143–174, 2002. 1

[2] P. Baker and Y. Aloimonos. Complete calibration of a multi-camera network. *Proc. IEEE Workshop on Omnidirectional Vision*, 12:134–141, 2000. 1

[3] P. Baker, A. Ogale, and C. Fermuller. The Argus eye: a new imaging system designed to facilitate robotic tasks of motion. *Robotics & Automation Magazine, IEEE*, 11(4):31–38, 2004. 1

[4] P. T. Baker and Y. Aloimonos. Calibration of a multi-camera network. *Conference on Computer Vision and Pattern Recognition Workshop*, 07:72, 2003. 1

[5] B. Caprile and V. Torre. Using vanishing points for camera calibration. *International Journal of Computer Vision*, 4(2):127–139, 1990. 1

[6] Y. Caspi and M. Irani. Aligning Non-Overlapping Sequences. *International Journal of Computer Vision*, 48(1):39–51, 2002. 2

[7] S. Dockstader and A. Tekalp. Multiple camera tracking of interacting and occluded human motion. *Proceedings of the IEEE*, 89(10):1441–1455, 2001. 1

[8] F. Dornaika. Self-calibration of a stereo rig using monocular epipolar geometries. *Pattern Recognition*, 40(10):2716–2729, 2007. 1

[9] R. I. Hartley and A. Zisserman. *Multiple view geometry in computer vision*. Cambridge University Press, ISBN: 0521540518, second edition, 2004. 1, 4

[10] R. Horaud and F. Dornaika. Hand-eye calibration. *International Journal of Robotics Research*, 14(3):195–210, 1995. 1

[11] M. Kaess and F. Dellaert. Visual SLAM with a Multi-Camera Rig. Technical report, Georgia Institute of Technology, 2006. 1

[12] T. Kanade, P. Rander, and P. Narayanan. Virtualized reality: constructing virtual worlds from real scenes. *Multimedia, IEEE*, 4(1):34–47, 1997. 1

[13] H. G. Maas. Image sequence based automatic multi-camera system calibration techniques. *In International Archives of Photogrammetry and Remote Sensing*, 32(B5):763–768, 1998. 1

[14] Z. Zhang. A flexible new technique for camera calibration. Technical report, Technical Report MSR-TR-98-71, Microsoft Research, 1998. 4

[15] Z. Zhang. A flexible new technique for camera calibration. *IEEE Transactions on Pattern Analysis and Machine Intelligence*, 22(11):1330–1334, 2000. 1, 6